Lasers in Medical Science (2022) 37:2033–2043
https://doi.org/10.1007/s10103-021-03466-z

ORIGINAL ARTICLE

Photoinactivation of multispecies cariogenic biofilm mediated by aluminum phthalocyanine chloride encapsulated in chitosan nanoparticles

Leonardo Lobo Ribeiro Cavalcante[1] · Antonio Claudio Tedesco[2] · Aline Evangelista Souza-Gabriel[1] · Hiago Salge Borges[2] · Fabiana Almeida Curylofo-Zotti[1] · Silmara Aparecida Milori Corona[1]

Received: 12 August 2021 / Accepted: 8 November 2021 / Published online: 23 November 2021

Abstract

This study aimed to characterize the aluminum phthalocyanine chloride (AlClPc) encapsulated in chitosan nanoparticles (CN) and apply it in antimicrobial photodynamic therapy (aPDT) on multispecies biofilm composed of *Streptococcus mutans*, *Lactobacillus casei*, and *Candida albicans* to analyze the antimicrobial activity and lactate production after treatment. Biofilms were formed in 24-well polystyrene plates at 37 °C for 48 h under microaerophilia. The following groups were evaluated ($n=9$): as a positive control, 0.12% chlorhexidine gluconate (CHX); phosphate-buffered saline (PBS) as a negative control; 2.5% CN as release vehicle control; the dark toxicity control of the formulations used (AlClPc and AlClPc + CN) was verified in the absence of light; for aPDT, after 30 min incubation time, the photosensitizers at a final concentration of 5.8×10^{-3} mg/mL were photoirradiated for 1 min by visible light using a LED device (AlClPc + L and AlClPc + CN + L) with 660 nm at the energy density of 100 J/cm^2. An in vitro kit was used to measure lactate. The biofilm composition and morphology were observed by scanning electron microscopy (SEM). The antimicrobial activity was analyzed by quantifying colony forming units per mL (CFU/mL) of each microorganism. Bacterial load between groups was analyzed by ANOVA and Tukey HSD tests ($\alpha=0.05$). A lower lactate dosage was observed in the aPDT AlClPc + CN + L and CHX groups compared to the CN and AlClPc groups. The aPDT mediated by the nanoconjugate AlClPc + CN + L showed a significant reduction in the viability of *S. mutans* (3.18 log10 CFU/mL), *L. casei* (4.91 log10 CFU/mL), and *C. albicans* (2.09 log10 CFU/mL) compared to the negative control PBS ($p<0.05$). aPDT using isolated AlClPc was similar to PBS to the three microorganisms ($p>0.05$). The aPDT mediated by the nanoconjugate AlClPc + CN + L was efficient against the biofilm of *S. mutans*, *L. casei*, and *C. albicans*.

Keywords Photochemotherapy · Chloro aluminum phthalocyanine · Mixed biofilm · Nanocarriers

✉ Silmara Aparecida Milori Corona
silmaracorona@forp.usp.br

Leonardo Lobo Ribeiro Cavalcante
leoloboribeiro@gmail.com

Antonio Claudio Tedesco
atedesco@usp.br

Aline Evangelista Souza-Gabriel
aline.gabriel@gmail.com

Hiago Salge Borges
hiago.s.borges@gmail.com

Fabiana Almeida Curylofo-Zotti
fabianacurylofo@gmail.com

[1] Department of Restorative Dentistry, Ribeirão Preto School of Dentistry, University of São Paulo (USP), Avenida do Café, s/n°, Monte Alegre, Ribeirão Preto, São Paulo 14040-904, Brazil

[2] Department of Chemistry, Center of Nanotechnology and Tissue Engineers, Photobiology and Photomedicine Research Group, FFCLRP—University of São Paulo (USP), Avenida do Café, s/n°, Monte Alegre, Ribeirão Preto, São Paulo 14040-904, Brazil

Introduction

The oral cavity is home to a great diversity of microorganisms that interact in a complex way.

[1]. The harmonic interaction of the commensal microbiome is responsible for maintaining homeostasis, which is fundamental for oral health. However, situations that interfere with the polymicrobial symbiotic relationship can cause part of the microbiota to grow and manifest pathogenic potential, leading to the development of oral diseases mediated by biofilms, such as periodontal diseases and dental caries [2]. Within a biofilm, each microorganism occupies a specific microenvironment, forming a complex and organized structure that makes them highly resistant [3].

Dental caries is a dynamic and multifactorial disease with a high prevalence worldwide [4]. Although children are more affected, it affects all age groups [5] and may progress to pulpitis, pulp infection, necrosis, abscess and, eventually, tooth loss [6]. *Streptococcus mutans* and *Lactobacillus* spp. were highlighted in studies due to their virulence factors, such as the acid by-product, arising from the metabolism of carbohydrates by these bacteria, which lead to demineralization of the tooth structure [6, 7]. However, instead of focusing on specific pathogens, the current paradigm of caries etiology emphasizes the mixed bacterial ecology, combined with behavioral, environmental, and immunological factors, as responsible for the onset of caries lesion and progression [8]. Furthermore, synergistic aggregates of bacteria and fungi are related to increased biofilm virulence, usually with a high *Candida albicans* count, especially in biofilms from children with early childhood caries [9].

The management of caries lesions depends on the extent, severity, and stage of the disease, always associated with measures to control causal factors to interrupt the disease process [8]. When they become cavitated, operative treatment with mechanical removal followed by restoration is indicated [10]. Appropriate decision on the amount of tooth tissue that should be removed by caries excavation is critical to avoid excessive removal of tooth structure [10] as recommended in the past. The minimally invasive philosophy proposes conservative approaches, such as selective caries removal, in which soft and moist dentin is preserved to avoid damage to the pulp and mitigate the risk of pulp exposure in deep lesions close to the vital pulp [11].

However, there are some controversial findings in the literature about this approach [11]. Although there is no increase in the number of bacteria close to the pulp after the peripheral sealing of the cavity with residual caries, it is not completely clear whether the remaining viable bacteria or their metabolites have a deleterious effect on the pulp [11]. There is insufficient high-quality clinical evidence to support that selective caries removal reduces the appearance of pulp complications and the risk of restoration failure [12].

This scenario implies complementary strategies to reduce the microbial load in the cavity after caries excavation to change the local cariogenic environment, interrupt the disease process, and, therefore, provide a more favorable biological condition for the longevity of restorations [13]. Agents as chlorhexidine, triclosan, and essential oils can reduce pathogens in the oral environment [7, 14]. However, the development of microbial resistance has restricted the use of these agents [15]. As an alternative, studies have shown that antimicrobial photodynamic therapy (aPDT) has positive results in reducing cariogenic microorganisms, without causing adverse effects to the pulp, even in more advanced stages of caries lesions, and with a low risk of microbial resistance [16, 17]. This treatment is based on the association of light sources with photosensitizing agents (PS), which, when irradiated in the presence of surrounding molecular oxygen, at a specific wavelength, are activated and undergo photochemical reactions in series with molecules close to them, by transferring electrons, generating free radicals (type I), or by energy transfer to oxygen (type II) that culminate in the production of singlet oxygen [16, 18]. Oxidative mechanisms that cause damage to the cell membrane, DNA, and protein/enzyme inactivation are mainly responsible for the lethality of microorganisms [18], even when arranged in biofilms [19].

Over the past few years, the search for new PS to achieve better antimicrobial efficacy of aPDT has been the subject of research [19]. Among the various classes of PS available, phthalocyanine derivatives have advantages due to their excellent absorbance in the visible red region of the light spectrum, high quantum yield of singlet oxygen generation, ease of physicochemical modifications, and stability [20]. Due to their high versatility, phthalocyanines, in special those with hydrophilic group or central metal ion on the original framework can easily combine with various drug delivery system to overcome limitations concerning their low solubility in aqueous or physiological media and high aggregation tendency that reduces their photodynamic potential [20]. Furthermore, relating phthalocyanine in nanodelivery systems based on polymers and nanoparticles with positively charged surface increases its interaction with the bacterial cell, an essential parameter to ensure greater efficacy of aPDT [21].

Chitosan nanoparticles (CN) can appropriately assume the role of phthalocyanine delivery system in aPDT against biofilms [22]. Chitosan is a biopolymer produced by the alkaline deacetylation of chitin present in the exoskeleton of crustaceans and the cell wall of fungi [23]. It emerged as

a drug delivery system mainly due to its biodegradability, biocompatibility, non-toxicity, and intrinsic antimicrobial activity [24]. Its mechanism of action is not fully understood but is mainly associated with changing the permeability of the negatively charged cell membrane to which polycationic chitosan is adsorbed, resulting in leakage of intracellular content [24]. This antimicrobial effect is enhanced when chitosan is in nanoparticulate form [24]. Therefore, to solve the mentioned limitations of phthalocyanine, it is expected that, when combined with CN, a dual antimicrobial activity will be reached. This study aimed to use more specifically aluminum phthalocyanine chloride (AlClPc) combined with CN to evaluate photoinactivation and lactate production from the multispecies biofilm of *Streptococcus mutans*, *Lactobacillus casei*, and *Candida albicans*.

Material and methods

Preparation of solutions

The CN were produced by the ionic gelation method with sodium tripolyphosphate (TPP) crosslinking. At room temperature, initially, 20 mL of Milli-Q water was placed in the 50-mL beaker, filtered through a 0.22 µm porosity filter, and 67 µL of glacial acetic acid (J.T. Backer, 100%, Phillipsburg, NJ, USA) was added, leaving the mixture under magnetic stirring for complete homogenization. Subsequently, chitosan (Sigma-Aldrich Co., St. Louis, MO, USA) was added 40.41 mg; the system was kept under constant agitation until complete dissolution of the solid. In another beaker, 2.0 mL of filtered Milli-Q water and 2.22 mg of sodium tripolyphosphate (TPP) were added, dissolving it with the aid of a tube shaker vortex until complete dissolution. After homogenization, the pH of the solution was determined and adjusted to 4.52. The mixture was filtered through a 0.45 µm porosity filter (vacuum filtration with a hydrophilic PTFE filter membrane, diameter 47 mm, pore 0.45 µm, plain white, non-sterile). Then, the nanoencapsulation of the AlClPc from an stock solution 1.0 mM (Sigma-Aldrich Co., St. Louis, MO, USA) in CN was obtained by a spontaneous emulsification process, as described above [25], with slight modifications. The final concentration of AlClPc + CN was 5.8×10^{-3} mg/mL (equivalent to 10 µM).

Characterization of photosensitizers

The characterization of the nanostructured compound was based on the analysis of particle size, polydispersion index (PdI), and zeta potential evaluated with the ZetaSizer nanoseries equipment (Malvern, Worcestershire, UK). The 10 µL volume of the samples was diluted in 1 mL of Milli-Q water in a 1 cm optical path polystyrene cuvette. Then, part of the solution was transferred to the model DTS1060 capillary cell (this analysis was performed after reading the sample size and PdI). The nanoparticle size and polydispersion index were obtained by photon correlation spectroscopy at 25 °C and scattering angle of 173°. The zeta potential, on the other hand, is reached due to electrophoretic mobility.

The spectroscopic analysis of the final solution was obtained by determination of the absorption spectra in a spectrophotometer (GE-Ultrospec 7000 GE Healthcare Life Sciences, Little Chalfont, UK) using 1 cm optical path quartz cuvettes with 2 polished faces and readings covering the wavelength range between 250 and 800 nm. To prepare the samples, 60 µL of the empty formulations (to be the blank) were aliquoted. Then, to "break" the nanoparticles, 60 µL DMSO (Sigma-Aldrich Co., St. Louis, MO, USA) was added, and the microtubes were placed in an ultrasonic bath (Bransonic Ultrasonic Cleaner—2210R-MTH) for 30 min. At the end, acetonitrile (J.T. Baker, 99%, Phillipsburg, NJ, USA) was added to complete the volumes of 1.5 mL in all microtubes, and readings were taken.

Light source

A continuous wave light-emitting diode (LED) irradiation device capable of photoirradiating the biofilms and simultaneously activating the AlClPc was self-manufactured. The equipment had a wavelength band center on 660 nm, composed of a current regulator, a digital life-time timer (Decorlux®, Curitiba, PR, Brazil) and an LED light source, in a flat shape of 14 × 10 LEDs (Cree®, Florianópolis, SC, Brazil). The light beam from the LED device was emitted from a distance of 8.3 cm from the biofilms for exposure. The power intensity of the LED light source was calibrated with a spectroradiometer (USB2000 +, Ocean Insight, Orlando, FL, USA) and set at 1.72 W/cm^2 on the plate surface. The irradiation spot size was adjusted to cover the 24-well culture plate. For the experiment, energy density was set at 100 J/cm^2 (precisely 103.2 J/cm^2) [26]. The irradiation time to reach the proposed dose was calculated using the classical equation where *energy density* (J/cm^2) = *intensity* (W/cm^2) × *time* (seconds), reaching 60 s of biofilm irradiation with single activation and no movement of the light source.

Culture media

Since we work with a mixed biofilm, selective culture media was required to cultivated each microorganism, allowing for subsequent individualized quantification of the colonies. For the growth of *S. mutans*, Mitis Salivarius Agar medium (Acumedia®, Neogen Corporation, Lansing, MI, USA) was prepared, supplemented with 20% sucrose, and added to 0.2 UI/mL of bacitracin and 200 UI/mL of Nystatin, in purified water. Agar Rogosa medium (BD Difco™, Sparks, MD,

USA) added with 200 UI/mL Nystatin and acetic acid was used to isolate *L. casei*. Sabouraud dextrose agar with chloramphenicol (Acumedia®, Neogen Corporation, Lansing, MI, USA) was used to cultivated *C. albicans*, with 65 g of the culture medium in 1000 mL of purified water, according to the manufacturer's instructions.

The Rogosa medium is not autoclavable, so the distilled water was autoclaved, and then the components of the medium were added in a sterile wood condition. The other media were autoclaved and placed in water bath until 75 °C to avoid denaturation of the nystatin proteins.

Multispecies biofilm growth

The multispecies biofilm was formed on polystyrene plates for cell cultivation from 24 wells (Kasvi®, São José do Pinhais, PR, Brazil). Plaques were pre-treated with human saliva donated by 5 adult volunteers with good systemic and oral health conditions and had not taken antibiotics in the previous three months. Salivation was stimulated by parafilm and collected in 50-mL tubes, centrifuged at 12,000 g for 20 min at 4 °C, and the supernatant filtered in a filtration system with a cellulose acetate membrane (0.22 µm) with the aid of a peristaltic pump for vacuum formation. A volume of 500 µL saliva was added to each well and incubated for 2 h at 37 °C. After this period, excess saliva was removed, leaving the biological film for biofilm formation.

The 24-well plates were inoculated with 1×10^7 CFU/mL *Streptococcus mutans* (ATCC 25,175), 1×10^7 CFU/mL *Lactobacillus casei* (ATCC 334), and 1×10^5 CFU/mL *Candida albicans* (ATCC 10,231) [27]. A spectrophotometer (Multiskan GO, Thermo Scientific Multiskan® Spectrum, MA, USA) was used to determine the cellular concentration of bacteria. The readings of bacterial suspensions in PBS were taken at 625 nm after calibration of zero absorbance. The concentration of *C. albicans* was determined in the Neubauer chamber due to the variability of morphology (hyphae or yeast) and cell size. After distributing 1.5 mL of the inoculum at the standardized concentration in each well, the plate was incubated at 37 °C in a microaerophilic environment, with stirring at 75 rpm for 48 h, in a bacteriological incubator (Shaker Incubator, Mod. CE-320, CienLab, Campinas, SP, Brazil) for biofilm formation and maturation.

Biofilm treatments

The 24-well plates were transferred from the oven to the laminar flow hood to perform the following biofilm treatments ($n = 9$): 0.12% chlorhexidine gluconate (CHX, positive control); phosphate-buffered saline (PBS; 100 mM NaCl, 100 mM NaH2PO4, pH 7.2, negative control); 2.5% nanoparticulated chitosan solution in acidic medium (CN, release vehicle control); aluminum phthalocyanine chloride solution in an organic medium in the absence of light (AlClPc, as a dark toxicity control of PS); aluminum phthalocyanine chloride encapsulated in chitosan nanoparticles in the absence of light (AlClPc + CN, dark toxicity control of encapsulated PS); aluminum phthalocyanine chloride with light incidence (AlClPc + L); and aluminum phthalocyanine chloride encapsulated in chitosan nanoparticles with light incidence (AlClPc + CN + L). All experiments were carried out in triplicate, at room temperature of 25 °C, and indirect natural lighting.

The inoculum was carefully removed by placing the pipette against the well wall. After removing the planktonic cells, 1 mL of the solutions was inserted. In the positive control, CHX remained in contact with the biofilm for 2 min. In the negative control (PBS) and release vehicle control (CN), the solutions were incubated with the biofilm for 30 min. AlClPc and AlClPc + CN solutions were inserted into the wells, followed by 30 min of incubation in light absence to verify the PS toxicity in the dark.

In another 24-well plate, antimicrobial photodynamic therapy was done using PS with the light source (AlClPc + L and AlClPc + CN + L). The incubation time of the PS was 30 min [26]. After this period, to allow the diffusion of PS through the biofilm and penetration into deeper cells, the biofilms with PS were light photoirradiated for 1 min.

Biofilm collection

At the end of the treatments, the solutions were removed, and two washes with PBS were carried out to remove any residue. Another 1 mL of PBS was added, and the biofilms were mechanically removed from the entire length of the well with the aid of a pipette tip and transferred to individually identified microtubes. Afterward, all the microtubes were taken to a vortex mixer (Phoenix Luferco, Araraquara, São Paulo, Brazil) for 30 s to homogenize suspension.

For sowing, 10 µL of the original biofilm solution was added to each of the three selective media mentioned above at zero dilution in Petri dishes. Then, decimal dilutions in sterilized PBS (10^{-1}, 10^{-2}, and 10^{-3}) were done to complete sowing. Finally, the plates were incubated in a microaerophilic environment at 37 °C for 48 h, the time necessary to determine the viability of the biofilm of *S. mutans* and *L. casei*, while *C. albicans* was incubated aerobically at 37 °C for 24 h.

Biofilm viability

The number of colonies obtained from sowing each dilution of each microorganism was counted with a stereoscopic magnifying glass (Carl Zeiss Microimaging GmbH, Göttingen, Germany), and the microorganism population count was expressed in colony-forming units (CFU/mL).

Lactate measurement

After the treatments, the biofilms were incubated in 1 mL of 5% sucrose solution in PBS in an oven at 37 °C. After 1 h, the volume of 10 µL of the suspension obtained from the biofilm was inserted together with 200 µL of enzymatic reagent containing lactate oxidase in the 96-well plate and incubated in the oven for another 5 min, according to the manufacturer's recommendations (Biotecnica Ltd, Varginha, Brazil). Finally, the reading was carried out in a spectrophotometer with a wavelength of 546 nm. Values were expressed in µmol/L and divided by time (minutes). The values were divided by biomass (quantified by absorbance) to obtain lactate secretion rates expressed as (µmol/L)/min/biomass [28].

Scanning electron microscopy (SEM)

For SEM analysis, samples were immersed in 2.5% glutaraldehyde for nine days and dehydrated in progressive ethanol concentrations (30%, 50%, 70%, 90%, and 100%). Afterward, the samples were fixed on metallic supports (stubs) and inserted into the camera for a critical drying point. After carbon evaporation, the samples were coated with a gold jet, visualized by SEM (Series EVO® 50, Carl Zeiss AG, Köln, Germany) in the SE (secondary electron) image acquisition mode and captured at 10,000 times magnification [22]. During the execution and analysis of SEM data, blinding was applied to the operator and analyst.

Statistical analysis

Data analysis was performed blinded by the data analyst (did not know the intervention in the groups) using the Statistical Package for Social Science for Windows (version 25; SPSS Inc, Chicago, IL, USA), with a significance level of 0.05. The normality of the count data of each microorganism was evaluated by the Shapiro–Wilk test presenting normal distribution (alpha = 0.05%) and analyzed by one-way analysis of variance (treatments) and by the complementary Tukey HSD test.

Results

Characterization of the photosensitizer

Characterization tests were carried out to verify the photophysical properties of the formulations at different periods. It was observed that the nanoparticles had an average size of less than 350 nm (Fig. 1A). The polydispersion index (PdI), which establishes the degree of homogeneity of the solution, obtained values between 0.42 and 0.45, indicating that the sample had values close to the acceptable standard (Fig. 1B). As expected, the zeta potential remained above + 30 mV at all follow-up periods, proving that the nanoconjugate was positively charged (Fig. 1C). The absorption spectrum, in triplicate, can be shown in the Fig. 2.

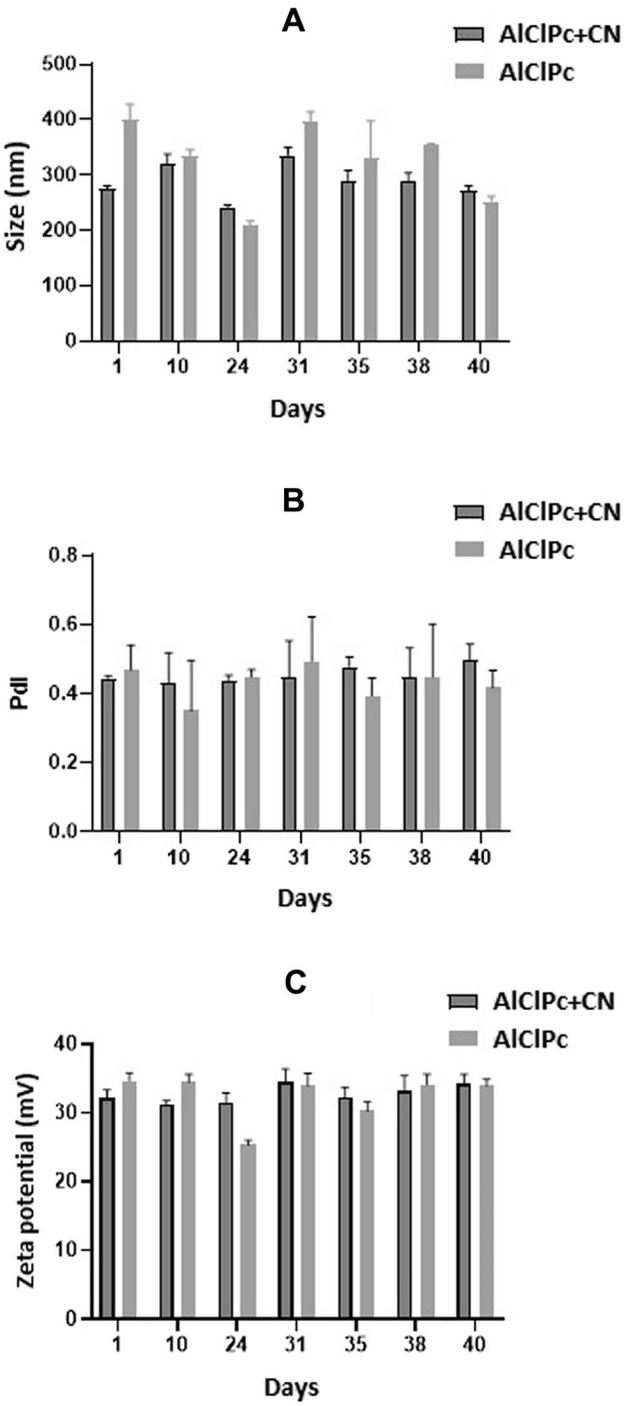

Fig. 1 Values of A sample sizes (nm), B polydispersion index (PdI), and C zeta potential (mV) of AlClPc + CN and AlClPc as a function of time (days)

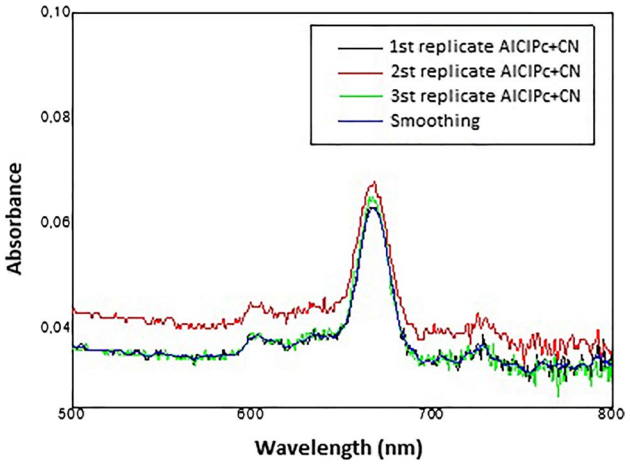

Fig. 2 Absorption spectra performed in triplicate

Lactate measurement

After validating properties, the nanoparticulate PS was used in aPDT on the multispecies biofilm. The lowest dosages of lactates were found in the groups AlClPc + CN + L and CHX compared to the other groups. The PBS, AlClPc + CN, and AlClPc + L groups showed intermediate results (Fig. 3).

Microbial viability

To assess the impact of aPDT on the viability of multispecies biofilm, the microorganisms *S. mutans*, *L. casei*, and *C. albicans* were cultivated together in the appropriate culture medium, and the experimental treatment and controls were applied. The quantification of viable colonies was performed for each microorganism by CFU/mL, and the results can be seen in Fig. 4. There was a significant reduction of *S. mutans* in treatments with AlClPc + CN + L, CHX, and CN compared to the other control groups ($p < 0.05$), showing a decrease of 3.18 log10 CFU/mL when comparing AlClPc + CN + L to the negative control PBS. In counting *L. casei*, CN promoted a significant reduction of viable colonies compared to CHX, PBS, AlClPc, and AlClPc + L, similar to AlClPc + CN. However, the greatest reduction was observed when using AlClPc + CN + L, statistically different from all groups ($p < 0.05$), with a decrease of 4.91 log10 CFU/mL of *L. casei* compared to PBS. The quantification of *C. albicans* showed a significant reduction of viable colonies with CHX and AlClPc + CN + L compared to the other groups, with a decrease of 2 log10 CFU/mL concerning PBS ($p < 0.05$).

Biofilm morphology

The SEM was performed to analyze the interrelationship of microorganisms in the multispecies biofilm and the implications of treatments on its morphology. The photomicrographs showed the growth of *S. mutans*, *L. casei*, and *C. albicans*, clearly distinguished, on the surface of the samples and the close relationship established between the three microorganisms (Fig. 5 A and B). The formation of exopolysaccharides was observed between the aggregated microcolonies in the samples from the control groups (Fig. 5C) and deformed cells, with membrane alterations in the group with experimental PS associated with light (Fig. 5D).

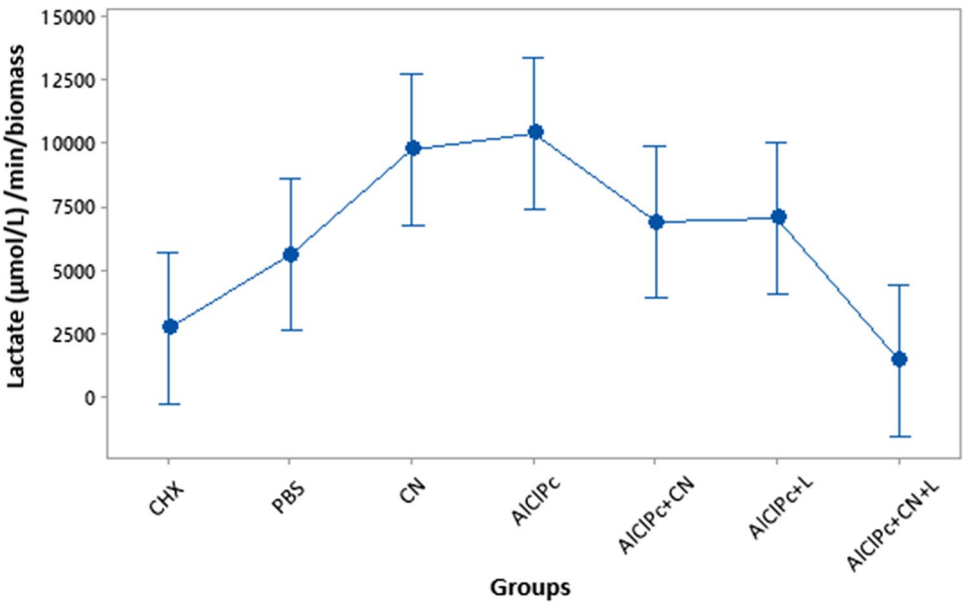

Fig. 3 Lactic acid production according to different treatments; errors bars: standard deviation. Tukey method and 95% confidence

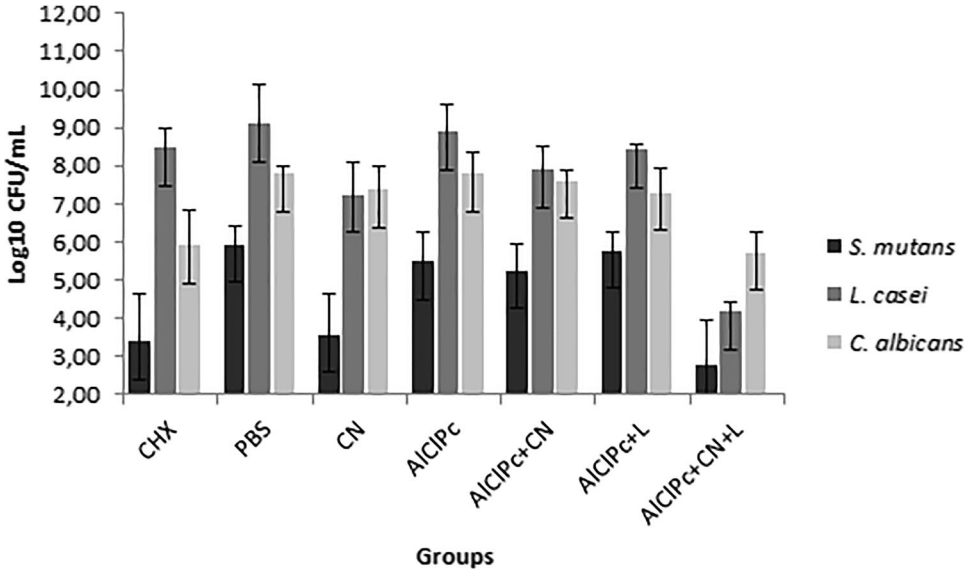

Fig. 4 Mean values of CFU/mL (log10) of multispecies biofilm composed by **A** *S. mutans*, **B** *L. casei*, and **C** *C. albicans* for different treatments; errors bars: standard deviation

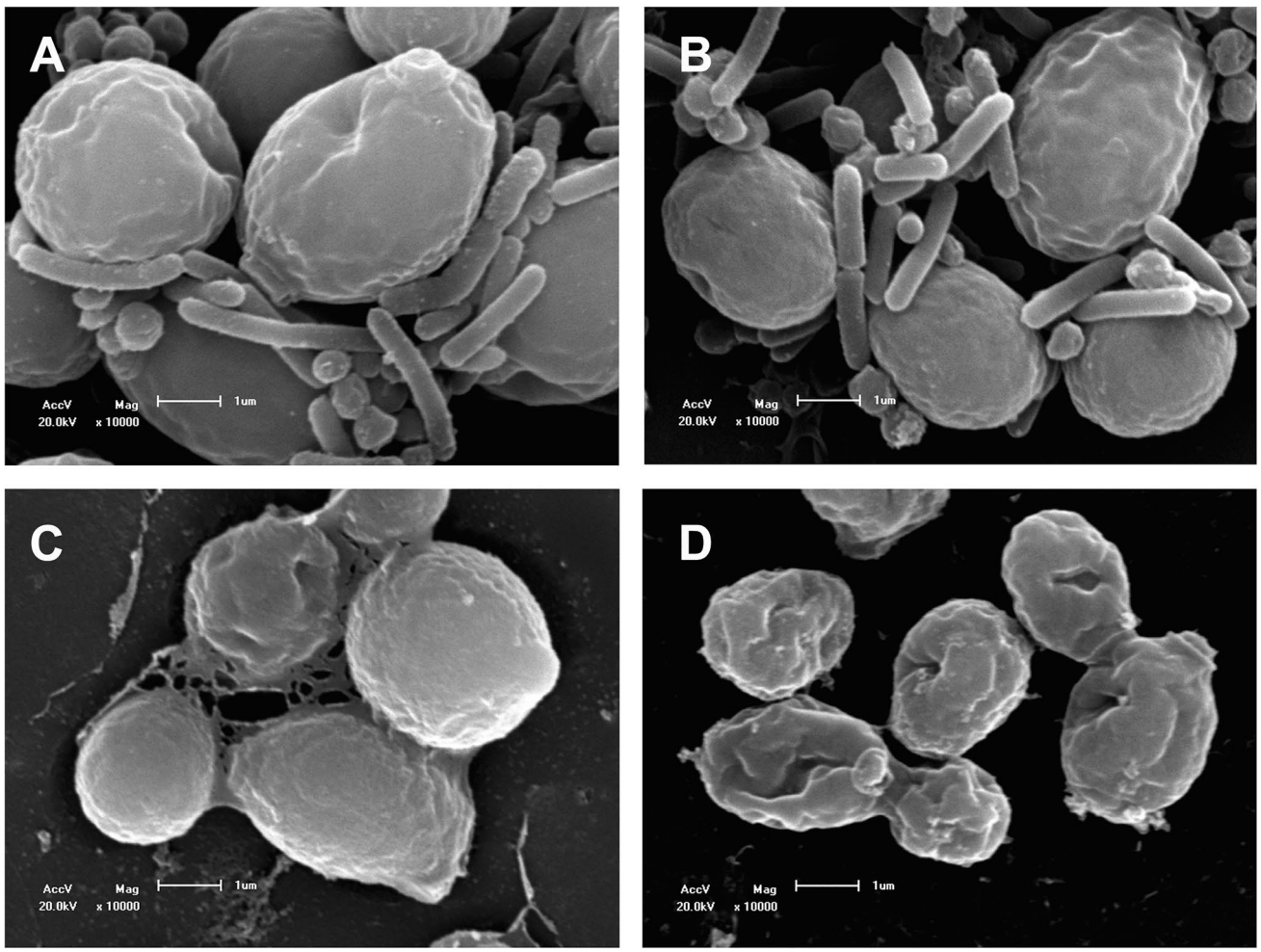

Fig. 5 Representative SEM photomicrographs of the multispecies biofilm. **A** PBS and **B** AlClPc groups show dense structure with clustered *S. mutans*, *L. casei*, and *C. albicans* cells. **C** AlClPc + CN group shows a microcolony incorporated in the extracellular polymer matrix. **D** AlClPc + CN + L group shows cells with membrane damage and appearance of emptying of the internal content. All images are shown at the same scale

Discussion

As caries is a disease of multifactorial etiology, the solutions to prevent its onset and progression also involve several factors, such as the control of cariogenic biofilm [8]. The gene expression of microorganisms in biofilms is different from the expression in their equivalent planktonic forms, and the collective production of extracellular matrices benefits the microbial community [3]. In this study, we mixed species of microorganisms to replicate the physiological heterogeneity, simulating an oral cariogenic biofilm.

We found that AlClPc + CN + L-mediated aPDT significantly reduced the viability of mixed biofilm composed of *S. mutans*, *L. casei*, and *C. albicans*. Other investigations have also found potential in aPDT to reduce mixed biofilm cell viability [19]. However, the multispecies biofilm is less susceptible to the antimicrobial action of the therapy when compared to the monospecies biofilm [29, 30], possibly due to its thickness and complexity [19]. It appears that the production and interaction of polymers from the matrix rich in extracellular polymeric substance (EPS) produced by interkingdom relationships result in increased matrix viscosity, developing resistance to disinfection in multispecies biofilms [29]. *C. albicans* is aciduric and acidogenic, and mainly when cultivated in biofilm with *S. mutans*, increases EPS production [9]. The higher amount of EPS can be explained by the finding that the glycosyltransferase B enzyme from *S. mutans* easily binds to the surface of *C. albicans* [31, 32] and activates the production of a glucan-rich matrix by the fungus, determining the virulence of cariogenic biofilms [33].

There is evidence that *C. albicans* and other yeasts, when subjected to aPDT, are more resistant to treatment than bacteria [29, 30, 34]. This finding agrees with our study in which despite having a significant reduction in *C. albicans*, the aPDT was more efficient in killing bacteria than *C. albicans* cells. This fact can be explained by structural differences such as nuclear membrane in yeasts, large cell size [29], and because gram-positive bacteria (as *S. mutans* and *L. casei*) are notably more sensitive to photodynamic inactivation due to a more porous cell wall [15]. However, when using a long incubation time with PS, there was a significant reduction in the metabolic activity of monospecies biofilms of *C. albicans*, *C. glabrata*, and *C. dubliniensis* [35].

The low permeability of PS by oral biofilm may constitute a limitation to using aPDT in caries treatment [15]. In a previous study of our research group, the parameters were similar to those used in this study, however, applied to the monospecies biofilm of *S. mutans* [22]. The reduction in microbial load compared to controls was smaller than that found in this multispecies biofilm study, probably due to differences in the incubation periods. While in the previous research, the pre-irradiation period was only 1 min, in this study, the time of PS diffusion through the biofilm was increased to 30 min, allowing a better PS capture by the biofilm, and therefore increasing the gradual release of PS by the nanoparticulate delivery system.

In addition to the incubation period, other factors can influence the efficiency of aPDT, such as the type of PS used. Several types of PS have been used for photoinactivation of multispecies biofilms in vitro [15]. Data available in Quishida et al. (2013) [34] showed that Photodithazine® activity on aPDT in *Candida albicans*, *Candida glabrata*, and *Streptococcus mutans* biofilms reduced cell viability by 1.21, 1.19, 2.39 log10, respectively, influenced, to some extent, by increasing the concentration of PS. The study by Trigo-Guierrez et al. (2018) [30] showed similar results in reducing the microbial load on the same biofilm model with aPDT mediated by AlClPc in cationic nanoemulsion but using only 39.9 J/cm^2. Another study that evaluated the antimicrobial efficacy of methylene blue on mature six species biofilms did not observe a reduction in the microbiota after a single application of the 60 s of aPDT [36]. In Gong et al. (2019) [37], the biofilm with *Streptococcus mutans*, *Lactobacillus casei*, and *Candida albicans* showed a significant microbial killing effect using erythrosine as PS. A dose-dependent effect was observed, that is, the reduction in colony quantification was proportional to the increase in energy dose. In our results, when using AlClPc + CN + L, the decrease in biofilm viability (*S. mutans*, *L. casei*, and *C. albicans*) compared with the negative control was 3.18 log10, 4.91 log10, and 2.09 log10, respectively. The PS encapsulated in CN was significantly more efficient in inactivating the biofilm than PS molecules in its isolated form, both irradiated with 100 J/cm^2 of energy dose. However, it is noteworthy that these studies used parameters different from those used in our study. It is likely that the variety of biofilm models and their degree of maturation, type of PS, concentration, release vehicle, incubation period, exposure time, and light energy dose have directly influenced the results of the studies [38]. The absence of a pre-established protocol for applying aPDT is a crucial issue to be considered in future investigations on biofilm photoinactivation.

To overcome hydrophobicity, a problem common to second-generation PS [39], we combined AlClPc with CN. This was expected to increase the solubility, avoid aggregation, ensure adequate photophysical and photochemical properties, and improve the photodynamic potential of AlClPc [22, 40]. Literature reveals the successful association of PS with nanocarriers used in aPDT [16, 22, 30, 39]. CN demonstrate broad-spectrum antimicrobial activity [41]. The production on a nanometric scale increases the reactive surface area of chitosan,

which is positively charged and interacts electrostatically with bacteria causing cell membrane destruction and death [42]. This result agrees with our outcome in which the CN were positively charged (zeta potential + 30 mV) and decreased *S. mutans* and *L. casei* compared to the controls. Furthermore, the results suggest a synergistic effect of AlClPc and CN in potentiating the antimicrobial activity of aPDT. However, CN did not demonstrate the same efficiency on *C. albicans*. In a previous study, chitosan solubilized in water had greater antifungal activity than chitosan dissolved in acetic acid, indicating that the dissolution medium influences the chitosan interaction with the yeast cell wall [43]. On the other hand, AlClPc without light incidence did not show cytotoxic for microorganisms, corroborating findings that show that AlClPc in the dark has no antimicrobial activity [26, 30].

The production of lactic acid by microorganisms of the cariogenic biofilm is directly associated with the demineralization/remineralization process [8]. In this sense, performing in vitro lactate measurements can increase the clinical relevance of studies investigating the control of this important virulence factor [44]. To the best of our knowledge, no previous study has done lactate analysis after using aPDT in cariogenic biofilms. Overall, the treatment with AlClPc + CN + L had a similar result to the positive control (CHX) and reduced acid production when compared to the other groups. Although there was a lactate reduction with the experimental PS, it was not compatible with the expressive decrease in the microbial load. Based on studies that used 3-h incubation [45], we believe that prolonging the biofilm incubation time with sucrose to allow higher acid production improved data fidelity.

Regarding clinical applicability, caries lesions are candidates for receiving aPDT as they are localized, with the direct action of the PS restricted to the caries site and access to lighting with light sources. However, the lack of standardization of the parameters used, the depth of radiation penetration in deep carious cavities, and the low selectivity of PS in microbial cells over host cells and tissue may be limiting factors for the therapy. In this study, a prolonged incubation period was used, which could affect clinically selectivity [18]. Despite this, other parameters used, such as the low concentration of PS, pronounced cationic charges, and its preference to accumulate in the cells of target microorganisms and the low irradiation time, improve selectivity [18]. Therefore, the main challenge now is to deliver the positive results of in vitro study under real conditions of action in the biofilm with efficacy and safety for patients in order to validate the use of this photosensitizing agent in clinical scenarios.

Conclusions

The biofilm formed by *S. mutans*, *L. casei*, and *C. albicans* was susceptible to aPDT mediated by the nanoparticle-based photosensitizer. Biofilm acidogenicity decreased, but not in proportion compatible with the reduction of microbial viability. AlClPc had enhanced efficacy when encapsulated in CN, suggesting a synergistic effect in the control of multispecies biofilm.

Funding This study was supported by the São Paulo Research Foundation (FAPESP) [grant number 2019/05965–0]. A.C.T and H.S.B also thank FAPESP [Thematic project #2013/50181–1] and the National Council for Scientific and Technological Development (CNPq) # 130399/2021–3 for the financial support.

Declarations

Conflict of interest The authors declare no competing interests.

References

1. Thurnheer T, Paqué PN (2021) Biofilm models to study the etiology and pathogenesis of oral diseases. Monogr Oral Sci 29:30–37. https://doi.org/10.1159/000510197
2. Mosaddad SA, Tahmasebi E, Yazdanian A, Rezvani MB, Seifalian A, Yazdanian M, Tebyanian H (2019) Oral microbial biofilms: an update. Eur J Clin Microbiol Infect Dis 38(11):2005–2019. https://doi.org/10.1007/s10096-019-03641-9
3. Davies D (2003) Understanding biofilm resistance to antibacterial agents. Nat Rev Drug Discov 2(2):114–122. https://doi.org/10.1038/nrd1008
4. Kazeminia M, Abdi A, Shohaimi S, Jalali R, Vaisi-Raygani A, Salari N, Mohammadi M (2020) Dental caries in primary and permanent teeth in children's worldwide, 1995 to 2019: a systematic review and meta-analysis. Head Face Med 16(1):22. https://doi.org/10.1186/s13005-020-00237-z
5. Kale S, Kakodkar P, Shetiya S, Abdulkader R (2020) Prevalence of dental caries among children aged 5–15 years from 9 countries in the Eastern Mediterranean Region: a meta-analysis. East Mediterr Health J 26(6):726–735. https://doi.org/10.6719/emhj.20.050
6. Karpiński T, Szkaradkiewicz A (2013) Microbiology of dental caries. J Biol Earth Sci 3:21–24
7. Choi O, Cho SK, Kim J, Park CG, Kim J (2016) In vitro antibacterial activity and major bioactive components of Cinnamomum verum essential oils against cariogenic bacteria, Streptococcus mutans and Streptococcus sobrinus. Asian Pac J Trop Biomed 6(4):308–314. https://doi.org/10.1016/j.apjtb.2016.01.007
8. Philip N, Suneja B, Walsh L (2018) Beyond Streptococcus mutans: clinical implications of the evolving dental caries aetiological paradigms and its associated microbiome. Br Dent J. 224(4):219–225. https://doi.org/10.1038/sj.bdj.2018.81
9. O'Connell LM, Santos R, Springer G, Burne RA, Nascimento MM, Richards VP (2020) Site-specific profiling of the dental mycobiome reveals strong taxonomic shifts during progression of early-childhood caries. Appl Environ Microbiol 86(7):e02825-19. https://doi.org/10.1128/AEM.02825-19

10. Kidd EA, Fejerskov O (2004) What constitutes dental caries? Histopathology of carious enamel and dentin related to the action of cariogenic biofilms. J Dent Res 83 Spec No C:C35–8. https://doi.org/10.1177/154405910408301s07
11. Schwendicke F, Frencken JE, Bjørndal L, Maltz M, Manton DJ, Ricketts D, Van Landuyt K, Banerjee A, Campus G, Doméjean S, Fontana M, Leal S, Lo E, Machiulskiene V, Schulte A, Splieth C, Zandona AF, Innes NP (2016) Managing carious lesions: consensus recommendations on carious tissue removal. Adv Dent Res 28(2):58–67. https://doi.org/10.1177/0022034516639271
12 Verdugo-Paiva F, Zambrano-Achig P, Simancas-Racines D, Viteri-García A (2020) Selective removal compared to complete removal for deep carious lesions. Medwave 20(1):e7758. https://doi.org/10.5867/medwave.2020.01.7758
13. Coelho A, Amaro I, Rascão B, Marcelino I, Paula A, Saraiva J, Spagnuolo G, Marques Ferreira M, Miguel Marto C, Carrilho E (2020) Effect of cavity disinfectants on dentin bond strength and clinical success of composite restorations-a systematic review of in vitro, in situ and clinical studies. Int J Mol Sci 22(1):353. https://doi.org/10.3390/ijms22010353
14. Santos A (2003) Evidence-based control of plaque and gingivitis. J Clin Periodontol 30(Suppl 5):13–16. https://doi.org/10.1034/j.1600-051x.30.s5.5.x
15. Silva Teófilo MÍ, de Carvalho RTMAZ, de Barros Silva PG, Balhaddad AA, Melo MAS, Rolim JPML (2021) The impact of photosensitizer selection on bactericidal efficacy of PDT against cariogenic biofilms: a systematic review and meta-analysis. Photodiagnosis Photodyn Ther 33:102046. https://doi.org/10.1016/j.pdpdt.2020.102046
16 Wilson BC, Patterson MS (2008) The physics, biophysics and technology of photodynamic therapy. Phys Med Biol 53(9):R61-109. https://doi.org/10.1088/0031-9155/53/9/R01
17. Reis ACM, Regis WFM, Rodrigues LKA (2019) Scientific evidence in antimicrobial photodynamic therapy: an alternative approach for reducing cariogenic bacteria. Photodiagnosis Photodyn Ther 26:179–189. https://doi.org/10.1016/j.pdpdt.2019.03.012
18. Hamblin MR (2016) Antimicrobial photodynamic inactivation: a bright new technique to kill resistant microbes. Curr Opin Microbiol 33:67–73. https://doi.org/10.1016/j.mib.2016.06.008
19. de Freitas MTM, Soares TT, Aragão MGB, Lima RA, Duarte S, Zanin ICJ (2017) Effect of photodynamic antimicrobial chemotherapy on mono- and multi-species cariogenic biofilms: a literature review. Photomed Laser Surg 35(5):239–245. https://doi.org/10.1089/pho.2016.4108
20. Ng DK (2014) Phthalocyanine-based photosensitizers: more efficient photodynamic therapy? Future Med Chem 6(18):1991–1993. https://doi.org/10.4155/fmc.14.139
21 Galstyan A (2021) Turning photons into drugs: phthalocyanine-based photosensitizers as efficient photoantimicrobials. Chemistry 27(6):1903–1920. https://doi.org/10.1002/chem.202002703
22. Cavalcante LLR, Tedesco AC, Takahashi LAU, Curylofo-Zotti FA, Souza-Gabriel AE, Corona SAM (2020) Conjugate of chitosan nanoparticles with chloroaluminium phthalocyanine: synthesis, characterization and photoinactivation of Streptococcus mutans biofilm. Photodiagnosis Photodyn Ther 30:101709. https://doi.org/10.1016/j.pdpdt.2020.101709
23 Kong M, Chen XG, Xing K, Park HJ (2010) Antimicrobial properties of chitosan and mode of action: a state of the art review. Int J Food Microbiol 144(1):51–63. https://doi.org/10.1016/j.ijfoodmicro.2010.09.012
24. Ma Z, Garrido-Maestu A, Jeong KC (2017) Application, mode of action, and in vivo activity of chitosan and its micro- and nanoparticles as antimicrobial agents: a review. Carbohyd Polym 176:257–265. https://doi.org/10.1016/j.carbpol.2017.08.082
25. Primo FL, Bentley MV, Tedesco AC (2008) Photophysical studies and in vitro skin permeation/retention of Foscan/nanoemulsion (NE) applicable to photodynamic therapy skin cancer treatment. J Nanosci Nanotechnol 8(1):340–347
26. Ribeiro AP, Andrade MC, Bagnato VS, Vergani CE, Primo FL, Tedesco AC, Pavarina AC (2015) Antimicrobial photodynamic therapy against pathogenic bacterial suspensions and biofilms using chloro-aluminum phthalocyanine encapsulated in nanoemulsions. Lasers Med Sci 30(2):549–559. https://doi.org/10.1007/s10103-013-1354-x
27. Yassin SA, German MJ, Rolland SL, Rickard AH, Jakubovics NS (2016) Inhibition of multispecies biofilms by a fluoride-releasing dental prosthesis copolymer. J Dent 48:62–70. https://doi.org/10.1016/j.jdent.2016.03.001
28. Rymovicz IUM, Ronsani MM, Grégio AMT, Guariza-Filho OG, Tanaka O (2013) Rosa EAR (2013) Virulence modulation of Streptococcus mutans biofilms by metal ions released from orthodontic appliances. Angle Orthod 83(6):987–993. https://doi.org/10.2319/112712-904.1
29. Pereira CA, Romeiro RL, Costa AC, Machado AK, Junqueira JC, Jorge AO (2011) Susceptibility of Candida albicans, Staphylococcus aureus, and Streptococcus mutans biofilms to photodynamic inactivation: an in vitro study. Lasers Med Sci 26(3):341–348. https://doi.org/10.1007/s10103-010-0852-3
30. Trigo-Gutierrez JK, Sanitá PV, Tedesco AC, Pavarina AC, Mima EGO (2018) Effect of Chloroaluminium phthalocyanine in cationic nanoemulsion on photoinactivation of multispecies biofilm. Photodiagnosis Photodyn Ther 24:212–219. https://doi.org/10.1016/j.pdpdt.2018.10.005
31. Falsetta ML, Klein MI, Colonne PM, Scott-Anne K, Gregoire S, Pai CH, Gonzalez-Begne M, Watson G, Krysan DJ, Bowen WH, Koo H (2014) Symbiotic relationship between Streptococcus mutans and Candida albicans synergizes virulence of plaque biofilms in vivo. Infect Immun 82(5):1968–1981. https://doi.org/10.1128/IAI.00087-14
32. Lobo CIV, Rinaldi TB, Christiano CMS, De Sales Leite L, Barbugli PA, Klein MI (2019) Dual-species biofilms of Streptococcus mutans and Candida albicans exhibit more biomass and are mutually beneficial compared with single-species biofilms. J Oral Microbiol 11(1):1581520. https://doi.org/10.1080/20002297.2019.1581520
33. Sampaio AA, Souza SE, Ricomini-Filho AP, Del Bel Cury AA, Cavalcanti YW, Cury JÁ (2019) Candida albicans increases dentine demineralization provoked by Streptococcus mutans biofilm. Caries Res 53(3):322–331. https://doi.org/10.1159/000494033
34. Quishida CC, Carmello JC, Mima EG, Bagnato VS, Machado AL, Pavarina AC (2015) Susceptibility of multispecies biofilm to photodynamic therapy using Photodithazine®. Lasers Med Sci 30(2):685–694. https://doi.org/10.1007/s10103-013-1397-z
35. Dovigo LN, Pavarina AC, Carmello JC, Machado AL, Brunetti IL, Bagnato VS (2011) Susceptibility of clinical isolates of Candida to photodynamic effects of curcumin. Lasers Surg Med 43(9):927–934. https://doi.org/10.1002/lsm.21110
36. Müller P, Guggenheim B, Schmidlin PR (2007) Efficacy of gasiform ozone and photodynamic therapy on a multispecies oral biofilm in vitro. Eur J Oral Sci 115(1):77–80. https://doi.org/10.1111/j.1600-0722.2007.00418.x
37. Gong J, Park H, Lee J, Seo H, Lee S (2019) Effect of photodynamic therapy on multispecies biofilms, including Streptococcus mutans, Lactobacillus casei, and Candida albicans. Photobiomodul Photomed Laser Surg 37(5):282–287. https://doi.org/10.1089/photob.2018.4571
38. Wilson M (1996) Susceptibility of oral bacterial biofilms to antimicrobial agents. J Med Microbiol 44(2):79–87. https://doi.org/10.1099/00222615-44-2-79

39. Zhang Y, Wang B, Zhao R, Zhang Q, Kong X (2020) Multifunctional nanoparticles as photosensitizer delivery carriers for enhanced photodynamic cancer therapy. Mater Sci Eng C Mater Biol Appl 115:111099. https://doi.org/10.1016/j.msec.2020.111099
40 Maldonado-Carmona N, Ouk TS, Calvete MJF, Pereira MM, Villandier N, Leroy-Lhez S (2020) Conjugating biomaterials with photosensitizers: advances and perspectives for photodynamic antimicrobial chemotherapy. Photochem Photobiol Sci 19(4):445–461. https://doi.org/10.1039/c9pp00398c
41. Ahmed ME, Mohamed HM, Mohamed MI, Kandile NG (2020) Sustainable antimicrobial modified chitosan and its nanoparticles hydrogels: synthesis and characterization. Int J Biol Macromol 1(162):1388–1397. https://doi.org/10.1016/j.ijbiomac.2020.08.048
42. Ibrahim H, El-bisi M, Taha GM, El-Alfy E (2015) Chitosan nanoparticles loaded antibiotics as drug delivery biomaterial. J Appl Pharm Sci 5:085–090. https://doi.org/10.7324/JAPS.2015.501015
43 Tayel AA, Moussa S, el-Tras WF, Knittel D, Opwis K, Schollmeyer E (2010) Anticandidal action of fungal chitosan against Candida albicans. Int J Biol Macromol. 47(4):454–457. https://doi.org/10.1016/j.ijbiomac.2010.06.011
44. Jiang W, Wang Y, Luo J, Li X, Zhou X, Li W, Zhang L (2018) Effects of antimicrobial peptide GH12 on the cariogenic properties and composition of a cariogenic multispecies biofilm. Appl Environ Microbiol 84(24):e01423-18. https://doi.org/10.1128/AEM.01423-18
45. Chen H, Zhang B, Weir MD, Homayounfar N, Fay GG, Martinho F, Lei L, Bai Y, Hu T, Xu HHK (2020) S. mutans gene-modification and antibacterial resin composite as dual strategy to suppress biofilm acid production and inhibit caries. J Dent 93:103278. https://doi.org/10.1016/j.jdent.2020.103278